

Radiation-induced absorption in bismuth-doped germanosilicate fibres

S.V. Firstov, V.F. Khopin, A.V. Kharakhordin, S.V. Alyshev, K.E. Riumkin,
M.A. Melkumov, A.M. Khagai, P.F. Kashaykin, A.N. Gur'yanov, E.M. Dianov

Abstract. We have investigated the effect of ionising radiation on the absorption properties of bismuth-doped germanosilicate fibres in the near-IR spectral region. Dynamic dependences of the changes in intensity and structure of the radiation-induced absorption spectra and the kinetics of its relaxation at various temperatures are obtained. A new absorption band is found in the wavelength region of 1.2 μm , which appears in irradiated high-germanium optical fibres doped with bismuth.

Keywords: bismuth, absorption, gamma irradiation, optical fibre, radiation-induced centres.

1. Introduction

It is known that the appearance of radiation-induced defects leads to an increase in optical loss in optical fibres, which reduces their throughput capability and narrows the range of potential applications (space industry, nuclear industry, etc.). A large number of papers have been published on this problem, in which the physical nature of such defects and the mechanisms of their formation have been comprehensively studied (see, for example, work [1] and references therein). As a result, it was shown that various defect centres caused by both the glass matrix itself and modifying additives (for example, Ge, P, Al) may be formed in the glass [2]. Optical properties and characteristic features of most such centres were studied in sufficient detail, which subsequently helped solve a number of practical problems, one of which was the increase in the radiation resistance of passive optical fibres [3–5].

The use of active optical fibres (with laser-active ions) in conditions of elevated radiation background is hampered by their higher sensitivity to ionising radiation compared to pas-

sive optical fibres [6, 7]. The reasons for this are different, in particular, the instability of active centers (as a result of photochemical reactions) under the influence of radiation or the appearance of new (caused by active ions or their clusters) radiation colour centers. Therefore, increasing the resistance of active optical fibres to ionising radiation is an important task of not only applied but also fundamental nature. It should be noted that the sensitivity of optical fibres depends on the active ion type; in particular, erbium fibres are more sensitive to radiation than ytterbium ones [8, 9]. It is known that the addition of Ce ions is used to increase the radiation resistance of optical fibres, including those doped with rare-earth ions (Er, Yb, Nd, etc.) [10, 11].

With the advent of new types of laser fibres, a need arises to study their sensitivity to ionising radiation. That is the reason why the present work is dedicated to the study of the effect of ionising radiation on optical characteristics in regard to new laser materials – bismuth optical fibres whose properties have not been sufficiently investigated. Interest in such optical fibres is stipulated by their ability to amplify optical radiation in the near-IR region, which makes it possible to use these optical fibres as active media in lasers, amplifiers and superluminescent sources. It is known that the introduction of bismuth into glass leads to the formation of various centres, which may have various effects on the radiation resistance of such optical fibres. Recently, the effect of the bismuth additive on the radiation resistance of erbium fibres has been investigated [12]. Our previous results have shown [13] that the sensitivity to the radiation of bismuth fibres depends to a large extent on the bismuth content in the glass matrix, even in spite of extremely small amount of bismuth (less than 10^{-3} mol %). In addition, it was established that at doses less than 10 kGy, there is no noticeable destruction of the bismuth active centres providing optical amplification.

The aim of this work is to study in detail the dynamics of radiation-induced absorption (RIA) and its relaxation in the spectral range of 900–1700 nm in germanosilicate optical fibres doped with bismuth at the temperatures from -60 to $+60$ °C.

2. Experiment

The experimental samples were segments of the single-mode germanosilicate (with different contents of germanium oxide in the core) bismuth-doped fibres. The designation and basic initial data on the investigated fibres are presented in Table 1. The fibres were drawn from preforms prepared by the method

S.V. Firstov Fiber Optics Research Center, Russian Academy of Sciences, ul. Vavilova 38, 119333 Moscow, Russia; Ogarev Mordovian State University, Institute of Physics and Chemistry, ul. Bolshevistskaya 6, 430005 Saransk, Russia, e-mail: fir@fo.gpi.ru;
V.F. Khopin, A.N. Gur'yanov G.G. Devyat'kh Institute of Chemistry of High-Purity Substances, Russian Academy of Sciences, ul. Tropinina 49, 603950 Nizhnii Novgorod, Russia;
A.V. Kharakhordin, S.V. Alyshev, K.E. Riumkin, M.A. Melkumov, A.M. Khagai, P.F. Kashaykin, E.M. Dianov Fiber Optics Research Centre, Russian Academy of Sciences, ul. Vavilova 38, 119333 Moscow, Russia

Received 15 September 2017; revision received 8 November 2017
Kvantovaya Elektronika 47 (12) 1120–1124 (2017)
Translated by M.A. Monastyrskiy

of modified chemical vapour deposition (MCVD). The outer diameter of the fibres was 125 μm , and the core diameter was 2–5 μm (at a cut-off wavelength $\sim 1.2 \mu\text{m}$). It is important to note that the bismuth-doped optical fibres being studied in this paper can be used to generate laser radiation in the spectral regions of 1350–1500 nm (No. 119) and 1650–1750 nm (No. 227).

Table 1. Designation and composition of the optical fibres under investigation.

Optical fibre No.	Glass composition/mol %	Bi content*(wt. %)
220	50GeO ₂ –50SiO ₂	absent
119	10GeO ₂ –90SiO ₂	0.01
227	50GeO ₂ –50SiO ₂	0.018

* Bismuth concentration was measured using inductively coupled plasma mass-spectrometry (ICP-MS).

As the main research method, the method of post-radiation chronospectroscopy was chosen, which consists in measuring the time dependences of the radiation induction and the relaxation of the optical losses of the samples. The fibres were irradiated with a gamma-source ⁶⁰Co (SRC ‘Kurchatov Institute’). Samples were placed at a certain (calibrated) distance from the source with the dose rate of about 1 Gy s⁻¹. To achieve a total dose of 1 kGy, the irradiation duration constituted ~ 1000 s. The post-radiation measurements were carried out for 2500 s. For fibre No. 227, additional RIA measurements were carried out at long time intervals after irradiation.

In all experiments, the intensity of the light signal $I(\lambda, t)$ passing through a segment of the test fibre of certain length was measured in the spectral range of 900–1700 nm at certain time intervals, starting from $t = 0$ (before irradiation), $0 < t < 1000$ s (during irradiation), and $1000 < t < 2500$ s (after irradiation). The fibre segment length (4–10 m) was chosen based on the absorption level in the IR region. The light signal source was an HL-2000 halogen lamp. The transmission spectra were recorded using an optical spectrum analyser (Ocean Optics NIR Quest). In carrying out temperature experiments, a thermostat was additionally used, maintaining the temperature from –60 to +60 °C with an accuracy of 5 °C. A detailed description of the measuring installation is given in [14].

The coefficient of radiation-induced absorption $\alpha(\lambda, t)$ (in dB m⁻¹) at the wavelength λ after time t from the irradiation onset was calculated by the formula

$$\alpha(\lambda, t) = -\frac{10}{L} \log\left(\frac{I(\lambda, t)}{I(\lambda, 0)}\right),$$

where $I(\lambda, 0)$ and $I(\lambda, t)$ are, respectively, the intensities of radiation that has passed through the optical fibre of length L (in meters) at the wavelength λ at $t = 0$ and after the time t from the irradiation onset.

As a result, the RIA spectra were determined for each sample. The estimate of induction and relaxation rates of RIA was carried out by constructing kinetic curves for different sections of these spectra. The comparison of such curves obtained for different optical fibres and temperatures made it possible to rank them by sensitivity to ionising radiation, depending on the selected conditions.

3. Results of experiments

Figure 1 shows the absorption spectra of the optical fibres under study. In the absorption spectrum of fibre No. 119 with a low content of germanium oxide, one can observe predominantly one brightly expressed band with a maximum at 1400 nm. In addition, for this type of fibres, small (less than 0.1 dB m⁻¹) optical losses are typical, with all other conditions being equal. An increase in the concentration of germanium oxide leads, firstly, to the appearance of a long-wavelength absorption band with a maximum at 1650 nm, and, secondly, to a noticeable increase in optical losses (fibre No. 227). As found in [15, 16], both absorption bands belong to bismuth active centres. From a comparison of the losses obtained for the bismuth fibre No. 227 and fibre No. 220 without bismuth (Fig. 1), it follows that bismuth makes a significant contribution to the magnitude of optical losses, since the glass matrix has sufficiently small intrinsic optical losses, which, at a wavelength of 1200 nm, are approximately fivefold less than in a bismuth-doped fibre. A significant increase in germanium oxide (from 10 to 50 mol %) also adversely affects the fibre’s optical losses, which is, apparently, due to the structural changes (defectiveness) of the glass network [17].

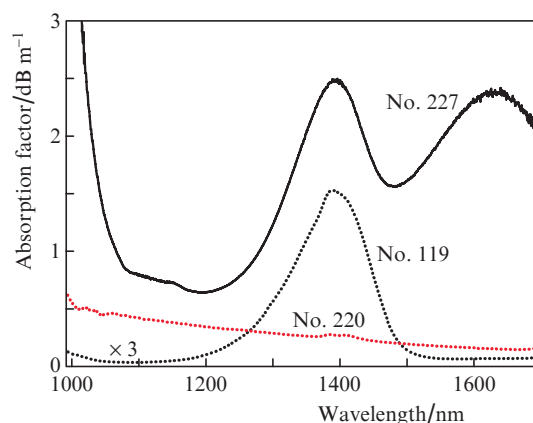


Figure 1. Absorption spectra of optical fibres under investigation. For the spectra indicated by the dashed curve, the absorption values are threefold increased for the convenience of comparison.

Figure 2 shows the RIA spectra of the investigated optical fibres. The spectra were measured during irradiation at the time moment corresponding to a total radiation dose of 1 kGy. Note one characteristic feature for all the presented fibres, which consists in a significant increase in the optical losses that occur upon irradiation. The spectrum shape of the irradiated fibre No. 220 is typical for such fibres [18]. The observed increase in optical losses is probably due to the presence of intense UV bands caused by radiation-induced defects, the long-wavelength edges of which extend to the near-IR region. From a comparison of the RIA spectra of fibres Nos 220 and 119, it can be concluded that the introduction of even a small amount of bismuth leads to a significant (four–fivefold) RIA increase. In a fibre with a high content of germanium oxide, in addition to the growth of optical losses, a new absorption band with a maximum of about 1200 nm appeared. Figure 2 (inset) shows this band obtained from the RIA spectrum of fibre No. 227 after the deduction of the

approximately threefold increased optical losses of the irradiated fibre No. 220. It should be noted that the appearance of this band is undoubtedly associated with the bismuth-radiation-induced centres, since it is absent in the absorption spectrum of a fibre without bismuth. On the other hand, in a bismuth fibre with a low germanium oxide content, this band is also not observed. The centres responsible for the detected band do not luminesce during optical excitation in the near-IR range.

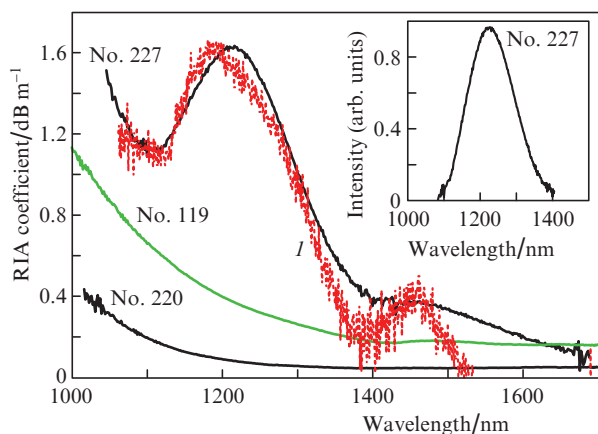


Figure 2. Typical RIA spectra at a radiation dose of 1 kGy. For comparison, photoinduced absorption spectrum (I) in the optical fibre No. 227 is shown when exposed to laser radiation with a wavelength of 532 nm. The inset shows a radiation-induced absorption band.

When analysing the data obtained, it was found that the shape and spectral position of the detected absorption band (Fig. 2, inset) coincide with the analogous parameters for the photoinduced band [photoinduced absorption spectrum (I) in Fig. 2] arising from the laser radiation with a wavelength of 532 nm [19]. In the same work, it was shown that this band is not connected with bismuth active centres.

Time dependences of the RIA change in the investigated optical fibres for the wavelengths of 1430 and 1600 nm (corresponding to absorption bands of bismuth active centres), and also of 1200 nm (a new absorption band) are shown in Fig. 3. For the measured dependences, typical is a sharp increase in absorption followed by a tendency toward saturation with increasing irradiation time (dose). With a good degree of accuracy, these dependences are described by a power function of the following form [20]:

$$\alpha = \delta D^\beta,$$

where α is the radiation-induced absorption (in dB m^{-1}); δ (in $\text{dB m}^{-1} \text{ Gy}^{-1}$) and β are the approximation parameters which depend on the fibre type under investigation; and D is the irradiation dose (in Gy) proportional to the irradiation time.

It is seen that the exponent β does not depend on the wavelength, in contrast to the parameter δ which, as expected, decreases with the wavelength. However, the exponent β equal to 0.77 for sample No. 220 turned out significantly less than that for fibres Nos 119 and 227, which amounted to 0.85. Most likely, this is due to the fact that, apart from the glass matrix, bismuth makes its own notable contribution to RIA.

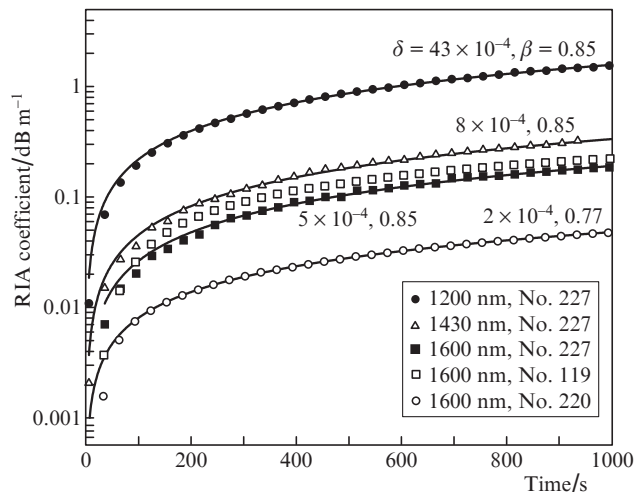


Figure 3. Typical temporal (dose) dependences of the radiation-induced absorption for various wavelengths (fibre No. 227). The approximation parameters δ and β are indicated near the corresponding curve; analogous dependences for fibres Nos 220 and 119 are given for comparison.

The post-radiation RIA measurements have shown that a slight decrease in RIA after irradiation is typical for all the fibres under study. Figure 4 shows the RIA relaxation kinetics for fibre No. 227. In the long-wavelength region ($\lambda > 1300$ nm), RIA is almost completely conserved, and in the short-wavelength range ($900 < \lambda < 1300$ nm) the RIA changes are most noticeable and may reach 15%.

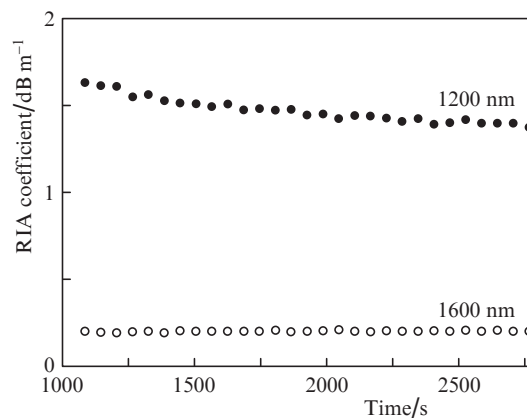


Figure 4. RIA relaxation kinetics (fibre No. 227).

Additional long-time measurements of RIA relaxation in the region of 1200 nm have shown a further monotonic decrease in absorption in this wavelength region. The experimentally obtained RIA relaxation kinetics of fibre No. 227 in the case of the extended time interval, which is presented in Fig. 5, is described by the formula [21, 22]:

$$\alpha = (\alpha_0 - \alpha_f)(1 + ct)^{-1/(n-1)} + \alpha_f,$$

where $c = (1/\tau)(2^{n-1} - 1)$; α_0 and α_f are the initial and final RIA values (in dB m^{-1}), respectively; τ is characteristic relaxation time; and n is a parameter that depends on the material and characterises the kinetics order.

Figure 5 shows the values of the main approximation parameters. The characteristic relaxation time at which the RIA is halved is about 2 hours. The exponent n characterising the kinetics order is close to three, which indicates the processes being more complicated than recombination of defects, oxygen vacancies and other interstitial centres with $n = 2$ (bimolecular processes). However, there are works (for example, [21]), which show that in some cases bimolecular processes may exist in glasses with the exponent $n > 2$.

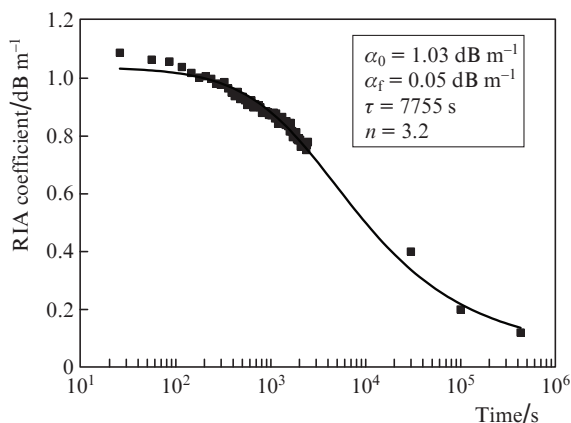


Figure 5. RIA relaxation kinetics at a wavelength of 1200 nm (fibre No. 227).

A series of temperature measurements (from -60 to $+60^\circ\text{C}$) of the RIA dynamics have allowed us to determine the rates of its growth at various temperatures. Figure 6 shows the dependence of the RIA induction rate on the value of T^{-1} at a wavelength of 1200 nm. The RIA guidance rate increases with temperature, but no significant changes are observed in the spectrum shape. Using the Arrhenius law, we have estimated the activation energy of this process as ~ 40 meV, which is comparable to the corresponding values for some glass network defects [23].

Nevertheless, our analysis of the temperature and time dependences of guidance and relaxation of the radiation-

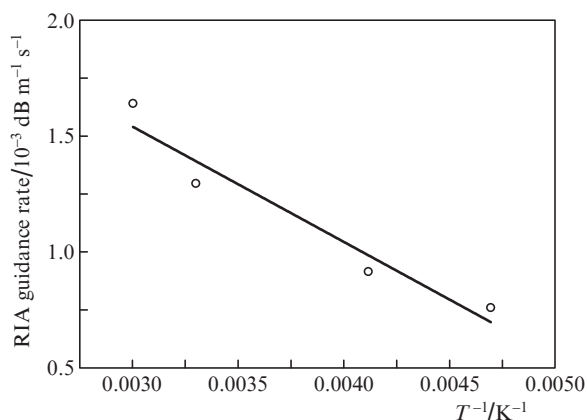


Figure 6. Dependence of the RIA induction rate on T^{-1} . Points are the experiment, and the straight line is the approximation by a linear function.

induced absorption band in the 1200 nm region shows that this band is most likely not exclusively connected with the glass network defects, but is stipulated by the presence of bismuth and the structural features inherent in germanosilicate glasses with a high content of germanium oxide.

4. Conclusions

Thus, the results of experiments on the effect of ionising radiation on the optical properties of bismuth optical fibres having a fused silica core with a high content of germanium oxide are presented. It is shown that while the concentration of bismuth is substantially lower than that of the remaining components of glass, its presence significantly increases the fibre sensitivity to ionising radiation. A comparative analysis of the RIA spectra for the fibres of various compositions has been carried out. As a result, a new absorption band with a maximum of about 1200 nm has been revealed, which occurs in the bismuth-containing fibres with a high content of germanium oxide under the action of gamma radiation. From the temperature and temporal dependences of induction and relaxation of the radiation-induced absorption band, the activation energy (~ 40 meV) of the defect centres responsible for the 1200 nm band and the kinetics order ($n \sim 3$) characterising the nature of the processes occurring in the glass are determined. It follows from the results obtained that this band cannot be exclusively attributed to the glass network defects or to bismuth active centres, but has a more complex nature.

Acknowledgements. The authors are grateful to A.L. Tomashuk for valuable discussions. The work was supported by the Russian Science Foundation (Grant No. 16-12-10230).

References

1. Pacchioni G., Skuja L., Griscom D. *Defects in SiO₂ and Related Dielectrics: Science and Technology* (USA, Norwell: Kluwer Academic Publishers, 2000).
2. Girard S., Tortech B., Regnier E., Van Uffelen M., Gusarov A., Ouerdane Y., Baggio J., Paillet P., Ferlet-Cavrois V., Boukenter A., Meunier J.P., Berghmans F., Schwank J.R., Shaneyfelt M.R., Felix J.A., Blackmore E.W., Thienpont H. *IEEE Trans. Nucl. Sci.*, **54** (6), 2426 (2007).
3. Lino A., Tamura J. *J. Lightwave Technol.*, **6**, 145 (1988).
4. Griscom D.L. *J. Appl. Phys.*, **78**, 6696 (1995).
5. Skuja L., Hirano M., Hosono H., Kajihara K. *Phys. Stat. Solid. C*, **1**, 154 (2005).
6. Zotov K.V., Likhachev M.E., Tomashuk A.L., Bubnov M.M., Yashkov M.V., Guryanov A.N., Klyamkin S.N. *IEEE Trans. Nucl. Sci.*, **55** (4), 2213 (2008).
7. Lezius M., Predehl K., Stöwer W., Türlér A., Greiter M., Hoeschen Ch., Thirof P., Assmann W., Habs D., Prokofiev A., Ekström C., Hänsch T.W., Holzwarth R. *IEEE Trans. Nucl. Sci.*, **59** (2), 425 (2012).
8. Henschel H., Kohn O., Schmidt H.U., Kirchhof J., Unger S. *IEEE Trans. Nucl. Sci.*, **45** (3), 1552 (1998).
9. Girard S., Ouerdane Y., Tortech B., Marcandella C., Robin T., Cadier B., Baggio J., Paillet P., Ferlet-Cavrois V., Boukenter A., Meunier J.P., Schwank J.R., Shaneyfelt M.R., Dodd P.E., Blackmore E.W. *IEEE Trans. Nucl. Sci.*, **56** (6), 3293 (2009).
10. Friebele E.J. *Appl. Phys. Lett.*, **27** (4), 210 (1975).
11. Girard S., Laurent A., Vivona M., Marcandella C., Robin T., Cadier B., Boukenter A., Ouerdane Y. *Proc. SPIE*, **7914**, 79142 (2001).
12. Sporea D., Mihai L., Neagu D., Luo Y., Yan B., Ding M., Wei Sh., Peng G.-D. *Sci. Rep.*, **6**, 29827 (2016).

13. Firstov S.V., Khopin V.F., Alyshev S.V., Firstova E.G., Riumkin K.E., Melkumov M.A., Khegai A.M., Kashaykin P.F., Guryanov A.N., Dianov E.M. *Opt. Mater. Express*, **6**, 3303 (2016).
14. Kashaykin P.F., Tomashuk A.L., Salgansky M.Yu., Guryanov A.N., Dianov E.M. *J. Appl. Phys.*, **121**, 213104 (2017).
15. Firstov S.V., Khopin V.F., Bufetov I.A., Firstova E.G., Guryanov A.N., Dianov E.M. *Opt. Express*, **19**, 19551 (2011).
16. Firstova E.G., Bufetov I.A., Khopin V.F., Vel'miskin V.V., Firstov S.V., Bufetova G.A., Nishchev K.N., Gur'yanov A.N., Dianov E.M. *Quantum Electron.*, **45** (1), 59 (2015) [*Kvantovaya Elektron.*, **45** (1), 59 (2015)].
17. Majérus O., Cormier L., Neuville D.R., Galois L., Calasa G. *J. Non-Cryst. Sol.*, **354** (18), 2004 (2008).
18. Regnier E., Flammer I., Girard S., Gooijer F., Achten F., Kuyt G. *IEEE Trans. Nucl. Sci.*, **54** (4), 1115 (2007).
19. Firstov S., Alyshev S., Khopin V., Melkumov M., Guryanov A., Dianov E. *Opt. Express*, **23**, 19226 (2015).
20. Liu D.T., Johnston A.R. *Opt. Lett.*, **19**, 548 (1994).
21. Griscom D.L., Gingerich M.E., Friebele E.J. *Phys. Rev. Lett.*, **71** (7) 1019 (1993).
22. Friebele E.J., Askins C.G., Shaw C.M., Gingerich M.E., Harrington C.C., Griscom D.L., Tsai T., Paek U., Schmidt W.H. *Appl. Opt.*, **30** (15), 1944 (1991).
23. Griscom D.L. *Appl. Phys. Lett.*, **71**, 175 (1997).